Heliyon 10 (2024) e37244

Contents lists available at ScienceDirect

Heliyon

journal homepage: www.cell.com/heliyon

Research article

Evaluation of thermal effects on urban road spatial structure: A case study of Xuzhou, China

Nana Guo [a], Xinbin Liang [a,*], Lingran Meng [b]

[a] College of Architecture, Anhui Science and Technology University, Bengbu, Anhui, 233000, China
[b] School of Geography and Tourism, Qufu Normal University, Rizhao, Shandong, 276800, China

ARTICLE INFO

Keywords:
Spatial nonstationary characteristics
Road network structure
Land surface temperature
Urban thermal environment
Geographically weighted regression
Spatial structure

ABSTRACT

Urban heat islands (UHI) are important environmental issue in cities where urban spatial structure has been proven to play an important role in alleviating UHI effects. The relationship between land surface temperature and urban spatial structures has been explored, providing strong support for their cooling effects. Urban roads are the skeleton of urban spatial structures, with obvious spatial structure characteristics; however, research on the relationship between roads and the thermal environment has been mostly focused at the micro and meso level, lacking exploration at the macro spatial structure scale. Xuzhou—a typical average-sized city in China—was selected as the research object and the road system as the carrier. The thermal environmental effects of road elements such as their structural attributes, geometric attributes and unique construction attributes were quantitatively analyzed using geographically weighted regression analysis. The results revealed that 1) the contribution of roads in the study area to the UHI effect is relatively stable; therefore, this area should become an important cooling space to decompose UHI patch connectivity and thus decrease the UHI effect. 2) the self-organizing structural characteristics of urban roads affect their thermal environments where in the straightness of the road structure and road thermal environment showed a clear overall negative correlation And 3) the length and width of the road segments had negative and positive effects on the thermal environment, respectively. The green coverage of the roads has a global negative effect on the thermal environment, but shows obvious spatial non-stationarity. Therefore, green measures must be implemented in different regions. The results here provide a quantitative basis for urban road system planning and urban form management and control that incorporates thermal environment improvements, as well as a reference for the study of urban thermal environments under different spatial forms and planning control systems in other countries and regions.

1. Introduction

Deterioration of the thermal environment is an important ecological issue in urban development. During urbanization, the urban spatial structure is constantly reconstructed along with the expansion of the urban geographic space [1]. Land use and transportation networks are decisive geographic representation elements that affect urban spatial structure [2–5]. As an important land use type and spatial carrier of the transportation network in a city, urban roads have a marked impact on urban thermal environment [4,6–8].

* Corresponding author.
E-mail address: liangxb@ahstu.edu.cn (X. Liang).

https://doi.org/10.1016/j.heliyon.2024.e37244
Received 26 April 2024; Received in revised form 21 July 2024; Accepted 29 August 2024
Available online 30 August 2024

Therefore, the analysis of the effect on thermal environment spaces of urban roads and quantification of thermal environment space planning strategies are important for optimizing urban thermal landscape patterns and improving the urban thermal environment.

Roads account for a large proportion of urban land use [9]; and with the expansion of cities, this proportion is in a steadily growing. Roads are covered by large amounts of impermeable materials and carry most of the automobile traffic in cities, making them critical urban heat sources [10,11]. Concurrently, urban roads serve as the main channels for organizing urban land use, connecting the functional zones inside the city and providing urban ventilation. Their structural forms also affect the thermal environment of an entire city by affecting other land uses and ventilation [12,13]. Currently, studies on the thermal environment effects of urban roads mainly include the thermal effects of the underlying surface material at the microscopic level [14–16] and the cross-sectional attributes of roads (road surface width and road green belts) at the mesoscopic level [17–20]. Most of these studies are limited to the road land use while studies on the effect of urban-road spatial structures on the urban thermal environment are lacking from the perspective of the role of roads in the overall urban structure.

The selection of appropriate indicators and methods to quantify and deconstruct the thermal environment effect of urban roads is important for mechanism investigation and scenario application, as is the clarification of the application points of strategic spaces [21]. Centrality is one of the key indicators for interpreting the spatial characteristics of road traffic networks [22], because it reflects the relationship between urban roads and land, the distribution characteristics of urban road centrality, and the structural characteristics of urban roads [5,23–25]. Remote sensing of land surface temperature (LST) is an important characterization parameter for analyzing urban thermal environment and has advantages in terms of spatial resolution and time continuity [26,27]. Ordinary least squares (OLS) regression is the most commonly used method, which assumes that all objects are independent but do not have a spatial scale effect [28]. In real geographic spaces, LST has a spatial autocorrelation, and to capture the effect of each influencing factor on LST at different spatial scales more accurately, it is necessary to perform a multiscale analysis based on spatial distribution [29,30].

To expand the study of the thermal environment effect of urban roads, the present study aimed to investigate the relationship between the geometrical and spatial structural characteristics of urban roads and LST. We selected Xuzhou, a typical Chinese city with an evident thermal environment, as our research object. We used Landsat satellite data and land use data for LST retrieval via the single-window algorithm and screened the indicators from the perspective of the geometric characteristics of urban roads and network centrality to quantify the characteristics of urban roads, test the LST spatial correlation of the road system, select a spatial regression model, and clarify the spatial non-stationary characteristics of LST under the influence of each indicator. These factors provide support for urban road optimization and can help expand research perspectives and ideas for improving the urban thermal environment at a holistic level.

2. Materials and methodology

2.1. Overview of the study area

Xuzhou is located in the northwestern Jiangsu Province and the southeastern North China Plain (33°43′–34°58′ N and 116°22′–118°40′ E). The city has an area of 11,258 km^2 and the study area—including Gulou, Quanshan, Yunlong, Tongshan, and New Districts as well as the Economic and Technology Development Zone— covers 573 km^2 and has an average elevation of 35.1 m (Fig. 1-a).The scope here included urban built-up areas, water bodies, suburban villages, agricultural and forestry lands and other land uses. Since the reform and opening up in China, road construction in the municipal district of Xuzhou has gradually improved. The per capita paved road area has increased from 1.00 m^2 in 1978 to 22.70 m^2 in 2021, and the paved road area has increased from 67 m^2 in 1978 to 4710 ha in 2021 (Fig. 1-b).Since Xuzhou resumed urbanization growth in 1995, its urbanization level increased from 19.8 % below the average level for both the world and China to 66.7 % higher than the average level for China in 2019. Despite the rapid urbanization and ecological construction transformation of resource-exhausted cities, there is still a notable heat island effect in the main urban area

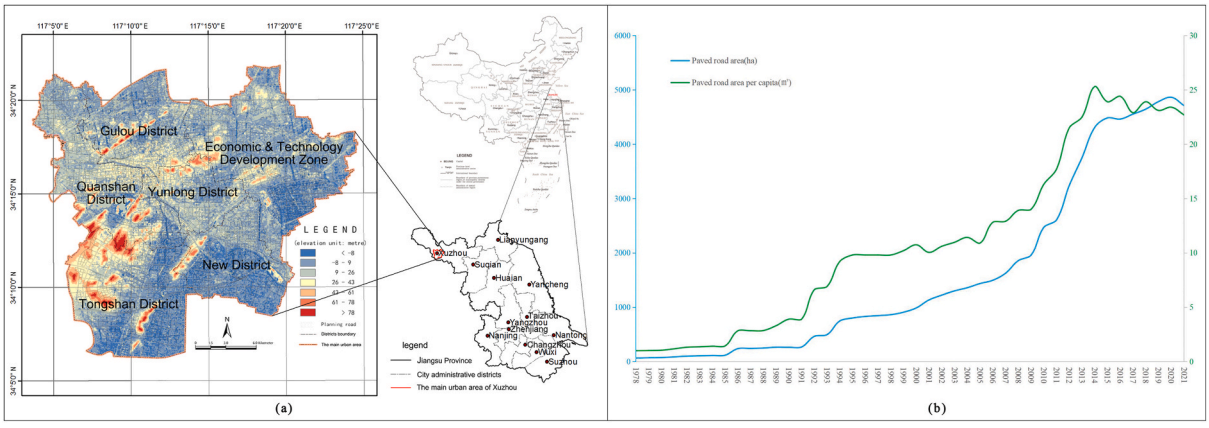

Fig. 1. Basic information of Xuzhou municipal districts: (a) location and (b) road construction in Xuzhou municipal districts over the years since the reform and opening up of China.

of Xuzhou [31].

2.2. Data source and processing

Comparing the characteristics of satellite image data commonly used in the study of heat island effects [32,33], and combining these with the accuracy requirements of this study, Landsat image data (basic parameters of the data source are shown in Table 1) from the Geospatial Data Cloud Platform of the Computer Network Information Center of the Chinese Academy of Sciences (http://www.gscloud.cn) were selected for the inversion of ground temperature. This included: Landsat 5 TM data of September 18th, 1995 with a rail number path of 121 and row of 36; Landsat 5 TM data of September 24th, 2003 with a rail number path of 121 and row of 36; and Landsat 8 OLI_TIRS data of September 22nd, 2014 and September 27th, 2019 with rail number paths of 121 and 122 and rows of 36 and 36, respectively. Other data included the urban master plan of Xuzhou City for each stage, the current land use maps of construction land in the main urban area of Xuzhou City (the years 1995, 2003, 2014, and 2019 were vectorized), and the administrative district map of Xuzhou City.

2.3. Research methods

2.3.1. Vegetation cover fraction (VCF)

The vegetation cover fraction (VCF) refers to the proportion of the vertical projection of vegetation to the area of the region. VCF is calculated mainly using the binary cell model combined with the vegetation index[34 [34], and the formula is as follows:

$$VCF = \frac{NDVI - NDVI_{soil}}{NDVI_{veg} - NDVI_{soil}} \tag{1}$$

where NDVI is the normalized difference vegetation index, and $NDVI_{soil}$ and $NDVI_{veg}$ are the NDVI of bare soil pixels and fully vegetated pixels, respectively; NDVI and VCF are the corresponding concepts. NDVI can reflect vegetation coverage, vegetation growth state, and nutritional information, and is an important parameter used to describe the ecological environment quality of a land parcel [35]. Based on the gray level of NDVI, the cumulative probabilities of 5 and 95 % of NDVI were used as the values of $NDVI_{soil}$ and $NDVI_{veg}$ respectively. The VCF values in the study area were calculated using ENVI software [36–38].

2.3.2. Measure of road space structure characteristics

Network centrality measurement is a way to analyze the structural characteristics of urban roads [39]. In practical applications, three indicators—Betweenness, Straightness, and Closeness—are used to describe the structural characteristics of roads [40,41] and have different meanings and focuses which can be used to judge the ability of roads in transit, directness, and accessibility, respectively [42]. Using the ArcGIS platform, Urban Network Analysis (UNA) [43] software was used to calculate the node centrality of the urban road network within the main urban area of Xuzhou. The indicators were as follows.

① Betweenness

This index is used to describe the urban road network centrality, Regarding road network consistency, the main factors affecting the number of betweenness for the urban road network nodes in the position, the more important the position of the node, the corresponding number of betweenness is greater, and the more paths related to it. For N road network nodes, the median is the ratio of the number of shortest paths between two nodes passing through node i and the number of all such paths, when making a comparative study of urban road networks of various scales, the influence of scale on the median should be eliminated, the common method is to introduce the coefficient 1/(N-1)*(N-2), Betweenness is then calculated using the following formula:

$$B_i = \frac{1}{(N-1)\times(N-2)} \sum_{\substack{j,k\in N \\ i\neq k\, j\neq k}} \frac{n_{jk}(i)}{n_{jk}} \tag{2}$$

where n_{jk} represents the number of shortest paths of nodes j and k, $n_{jk}(i)$ represents the number of paths passing through i, and N represents the number of road network nodes.

② Straightness

Table 1
Road section parameters of main urban area over the years.

Year	Amount	Shortest (km)	Longest (km)	Totle (km)	Average (km)	Std dev	Density (km/km^2)
1995	330	0.10	8.42	380.41	1.15	1.12	0.66
2003	1766	0.02	9.12	853.80	0.48	0.65	1.49
2014	2840	0.01	4.30	1202.25	0.42	0.42	2.10
2019	3721	0.02	4.77	1499.13	0.40	0.39	2.62

Straightness indicates the efficiency of urban road network—in the same urban road network, the size of the value of direct access is related to its position in the urban road network. In the process of quantitative analysis, mainly through the road network of a node i and the nodes of the spacing and the shortest spacing of the ratio of the road network. For the different scales of the urban road network for comparative study, the scale of the impact of direct access should be eliminated, and the common method is to introduce the coefficient of 1/(N-1) into the formula as follows:

$$S_i = \frac{1}{N-1} \sum_{j \in N,\ j \neq i} \frac{d_{Euclij}}{d_{ij}} \tag{3}$$

where d_{ij} is the distance between the nodes i and j in the network, d_{Eculij} is the Euclidean distance between them, and N is the number of nodes in the road network.

③ Closeness

This indicator reflects the proximity of a node. It is specifically expressed as the reciprocal of the mean value of the path length between node i and every other node in the road network and can be determined using the following formula:

$$C_i = \frac{1}{L_i} = \frac{N-1}{\sum_{j \in G} d_{ij}} \tag{4}$$

where L_i is the mean value of the distance between node i and other nodes, and d_{ij} corresponds to the distance between these two nodes.

④ Dual graph

Certain connections between the dual and planar graphs create a special network, the result of appropriately processing the dual relationships of different nodes and edges in the planar graph. For example, in dual processing, a point on each edge in a planar graph network can be selected as a vertex in the dual graph, and the edges and vertices are connected in a certain order to form the corresponding graph. An analysis shows that the new graph, which is composed of these vertices and links, contains the connection relationship of the original planar graph, which is called a dual graph or the dual structure of the original planar graph (Fig. 2).

The dual graph retains the overall morphological characteristics and visually reflects the connectivity of the road segments. Usually, the urban road network uses intersections as the nodes and the solid linear road segments as the edges, thus corresponding to the shape of the road network in a real environment and essentially reflecting the interconnection status of the intersections of urban road segments. To quantitatively analyze the spatial structural attributes of a road segment, dual graph analysis can be used to abstract a single road segment as a single node according to the spatial connection relationship between each road segment; thus, a dual graph of the urban road network can be constructed to express the abstract attributes of each road segment in the urban road network structure [44].

2.3.3. Geographically weighted regression analysis

To better explain the nonstationary pattern of LST, geographic weighted regression (GWR) analysis was introduced, and the geographic location information of the spatial data was embedded into parameters to reflect the relationship between variables and their spatial variation characteristics [45].

However, the traditional GWR model has certain limitations. The model assumes that all independent variables affect the dependent variable at the same spatial scale; and ignores the adaptation range of spatially independent variables. Therefore, we added

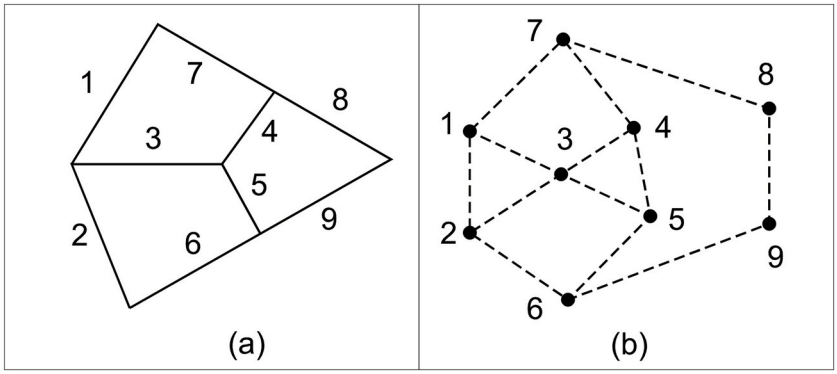

Fig. 2. Illustrations of Plane graph and dual graph of the road network structure (a) planar graph; (b) dual graph.

a multiscale GWR to strengthen the adaptability of spatially independent variables [46]. The adaptability (y_i) of the OLS, GWR, and multiscale geographic weighted regression (MGWR) models to the nonstationary thermal environment in the main urban area of Xuzhou were compared to fully evaluate the explanatory power of each model using the following equation:

$$y_i = \beta_0(u_i, v_i) + \sum_{k=1}^{p} \beta_k(u_i, v_i) x_{ik} + \varepsilon_i \tag{5}$$

where p is the number of selected road thermal environment influencing factors ε_i is a random error. (u_i, v_i) is the geospatial coordinates of the center point of road segment i, $\beta_0(u_i, v_i)$ is the intercept at road segment i, and $\beta_k(u_i, v_i)$ is the regression coefficient of the k-th indicator on road segment i, of which $\beta_0(u_i, v_i)$ and $\beta_k(u_i, v_i)$ are estimated using the linear weighted least squares method:

$$\widehat{\beta}(u_i, v_i) = \left[X^T W(u_i, v_i)\right]^{-1} X^T W(u_i, v_i) Y \tag{6}$$

where X is the independent variable matrix, Y is the dependent variable matrix, $W(u_i, v_i)$ is the spatial weight matrix, and the bisquare is selected as the weight function:

$$W_{ij} = \begin{cases} \left[1 - (d_{ij}/b)^2\right]^2, d_{ij} \le b \\ 0, others \end{cases} \tag{7}$$

where W_{ij} is the weight influence between the road segments i and j, d_{ij} is the Euclidean distance between the road segments i and j, and b is the bandwidth.

Because the spatial distribution of road segment center points in the study area is non-uniform, the adaptive type was chosen in this section; that is, the distance between the regression analysis road segment i and the M-th nearest neighbor was used as the bandwidth [47]. M is determined by the Akaike information criterion and the bandwidth value is characterized by M [48]. The bandwidth is negatively correlated to the rate at which the weight decays with increasing distance [47]. A bandwidth that is too large may also lead to globalization trend in the GWR model. In short, the scale of action of the independent variable on the dependent variable can be reflected by the bandwidth.

3. Results

3.1. Road characteristics

Current land use maps of Xuzhou's main urban area over the years were used to extract the land use for each level of road land, extract and decompose the road centerline of each level of road, and draw the road segments of the main urban area of Xuzhou over the study period (Fig. 3-a).

From 1995 to 2020, the road network in the main urban area of Xuzhou improved constantly. Specifically, in 1995, the road network of the main urban area as a whole was internally dense and externally sparse, with the old urban area as a single center. In

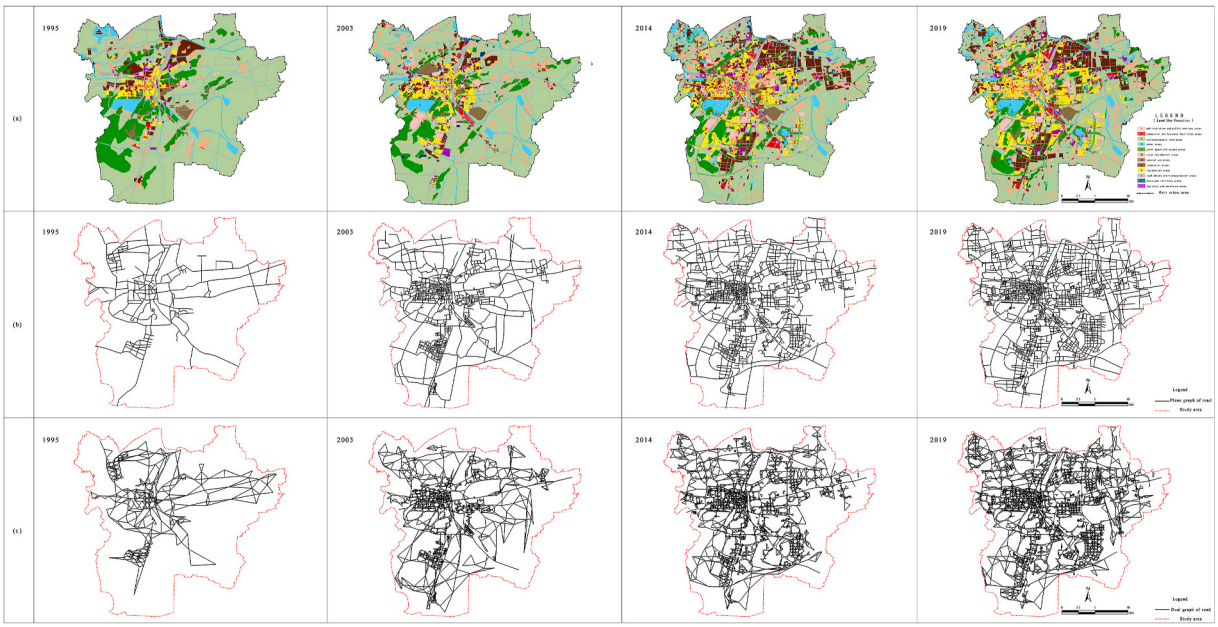

Fig. 3. Road network structure of Xuzhou City in 1995, 2003, 2014 and 2019. (a) Land use; (b) Planar graph; (c) Dual graph.

2003, the road network in the main urban area gradually improved, and road density increased. The road network in the Tongshan District and the area north of Daguozhuang Airport was strengthened, and a dense road network centered on the old town and Tongshan District emerged. By 2014, the road network of the Xuzhou New District in the main urban area had been constructed. The old city, Tongshan District, and Xuzhou New District became the centers of the multi-center dense road network structure, and the framework of the road network system was relatively mature. By 2019, the road network structure—characterized by the original three centers, which were internally dense and externally sparse—began to evolve into a road network system with a relatively homogeneous space, and the road network was gradually constructed and improved. In ArcGIS, the parameters of each road segment over the years were counted to obtain a parameter table for the road segment in the main urban area (Table 1).

Table 1 shows that the number of road segments increased from 330 in 1995 to 3721 in 2019; the total number of road kilometers increased from 380.41 km in 1995 to 1499.13 km in 2020; the density of the road network also increased from 0.66 km/km^2 to 2.62 km/km^2, and the efficiency of the road system increased.

In ArcGIS, in accordance with the principle shown in Fig. 2 and combined with road segment modifications such as expressways and interchanges, dual graphs of the road centerlines in the main urban area of Xuzhou from 1995 to 2020 were drawn (Fig. 3-b). The graphs show a clear group pattern from a single center to multiple centers; and with the gradual construction of the road network system, the group-type centralized distribution characteristics of polycentricity became obvious. Among these, the new district and the old urban area of Xuzhou are the two larger and more concentrated distribution areas.

3.2. Road VCF characteristics

In addition to the influence of location, the construction of urban roads affects the LST of road segments because of road width and road greening. As well as the analysis of urban space planning factors in Section 3, VCF was selected as an important independent variable in the correlation analysis. In ArcGIS, the VCF data of the main urban area and the road segments were superimposed to extract the VCF value of each road segment (Fig. 4).

Based on the VCF statistics of each road segment over the years, the average values for the four periods were 0.41, 0.28, 0.32 and 0.34, respectively. A combination of the spatial distribution of road segments over the years in Fig. 3-a indicates that before 2003—with the improvement of the road system and the increase in the construction of road segments—the VCF showed a decreasing trend, and the reduction rate was relatively large. The space showed a clear circular structure; that is, the VCF gradually increased from the urban center to the periphery. After 2003, although the construction volume of road segments increased, the VCF of roads also exhibited an increasing trend. Among them, the VCF of the main expressways in the non-transit urban area was low, especially on the eastern and western third-ring roads and Chengdong Avenue.

3.3. Road structural characteristics

The centrality and spatial structural characteristics of roads in the main urban area were determined. Formula 2, 3 and 4were used to calculate road centrality. We also conducted statistical analyses on the basic status of the road network in the main urban areas of Xuzhou over time (Table 2).

As shown in Table 2, the number of road dual graphs gradually increased from 1476 in 1995 to 15,956 in 2019, indicating that the road network became more closely connected and complicated. The changes in the overall normalized straightness and normalized closeness exhibited dynamic trends. The normalized mean betweenness showed a clear decreasing trend. Because the network parameters and network size had a certain correlation between 1995 and 2020, the network size changed greatly, therefore, we compared the network centrality parameters of single-period data. Based on the calculation results of the UNA and ArcGIS platforms, the network centrality parameters of the 1995–2020 road centerline dual graph for the main urban area of Xuzhou were classified using the natural discontinuity method. A spatial structure characteristic map of the road space in the main urban area of Xuzhou over the years was drawn (Fig. 5).

As shown in Fig. 5, the road network centrality parameters of the main urban area of Xuzhou show clear spatial differentiation characteristics over time. Betweenness centrality reflects the distribution characteristics of typical planar aggregations that extend in the axial direction. In 1995, road segments with higher betweenness centrality were mainly distributed in the old urban area and Tongshan District (formerly Tongshan County). By 2019, the main frame of the road segments with high betweenness centrality had expanded along the main roads, and the space exhibited the multi-region coexistence of the old city, Xuzhou New District and Chengdong New District (Xuzhou Economic Development Zone). Road segments with low betweenness centrality were distributed in

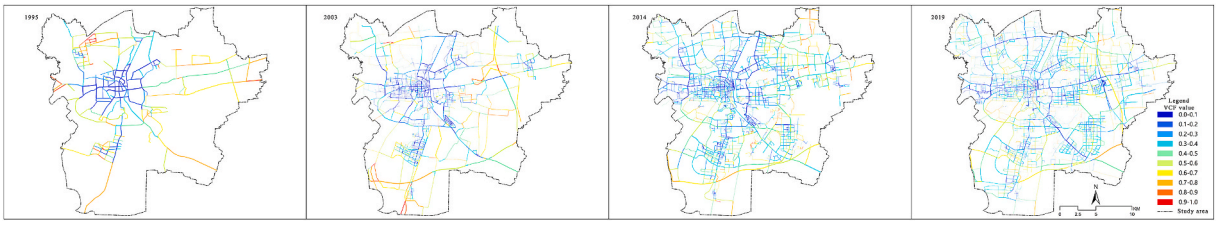

Fig. 4. VCF of various road sections in the main urban area of Xuzhou.

Table 2
Statistics of the basic conditions of the road network in the main urban area of Xuzhou.

Year	Dual number	Norm_Betweenness	Norm_Straight	Norm_Closeness
1995	1476	3.21e-2	0.86	0.10 e−3
2003	7432	1.61 e−2	0.83	0.14 e−3
2014	11926	1.18 e−2	0.83	0.13 e−3
2019	15956	0.97 e−2	0.86	0.12 e−3

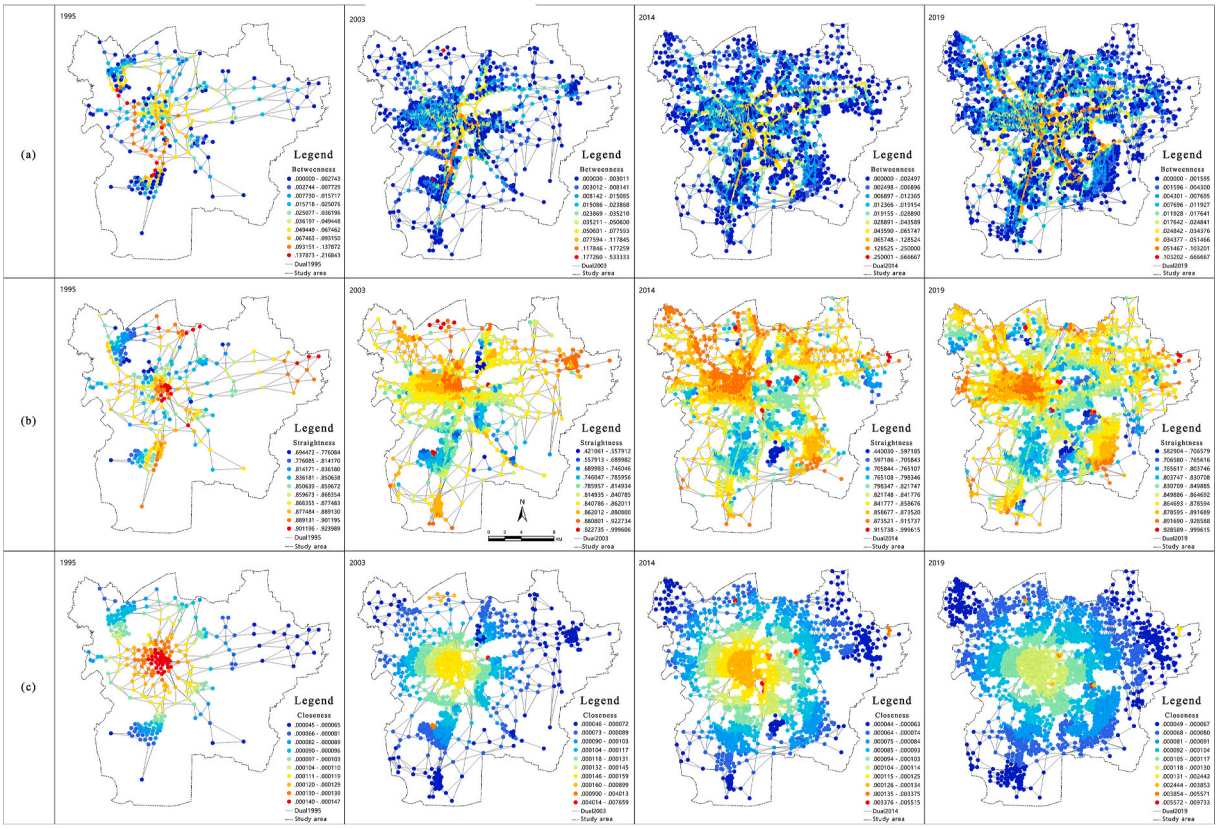

Fig. 5. Spatial structure characteristics of roads in the main urban area of Xuzhou (a) Betweenness; (b) Straightness; (c) Closeness.

the surrounding area. In general, the higher the betweenness value, the higher the number of shortest road paths passed by the nodes of the road traffic network, the larger the traffic flow carried in the corresponding road network, and the better the accessibility [49]. The spatial expansion of the high-betweenness central road segment showed a certain degree of fit with the development of urban land use, particularly with the urban skeleton formed by the main roads.

The straightness of the road network in the main urban area of Xuzhou City over the years shows a clear group structure that reflect the transportation network efficiency to a certain extent. In 1995, areas with higher straightness appeared in the vicinity of Xuzhou Station in the main urban area, the Wanzhai Port area of Xuzhou North Station, and the area of Damiao Town, while the weakest area appeared in southern of Jiuli Lake. By 2003, the overall pattern began to show clear zoning characteristics, with areas of high straightness mainly concentrated in the commercial area west of Xuzhou Station and the residential area on the north bank of Yunlong Lake. In 2014 and 2019, the zoning exhibited clear polycentric characteristics With the new and old urban areas of Xuzhou exhibiting the highest straightness. The straightness south of Tuolong Mountain was the weakest because the vicinity of Xuzhou Station and the north bank of Yunlong Lake are old historical urban areas, the spacing of their road network is relatively small, and the network connectivity is stronger at the same spatial scale. The base road networks were reorganized and constructed in Xuzhou New Urban Area in accordance with the new planning, there was no interference from the old road network, the road system was complete, and the hierarchical system was clear. The evaluations of road network structures in new urban areas based on straightness reflects the rationality of road network structures in new urban areas.

The proximity of the road network in the main urban area of Xuzhou City over the years showed a clear circular structure in which the old urban area (Xuzhou Station) was the center, and the roads expanded outward. Closeness reflects the proximity of each network node to the road network center. The higher the closeness, the closer the node is to the network center. For the road network as a

whole, the higher the total closeness, the denser the road network structure. The center of the network structure of Xuzhou is still based at Xuzhou Station in the main urban area and the commercial concentration area on the west side, with strong centrality. In ArcGIS, the total closeness values for 1995, 2003, 2014, and 2019 were 0.000105, 0.002553, 0.002636, and 0.026685, respectively. The closeness of the main urban area shows an increasing trend; that is, the road network structure became increasingly dense with the increase in road network construction in the main urban area.

3.4. Road thermal environment

Road networks are one of several urban network frameworks, and the thermal environment of these networks is affected by their spatial structure. For example, the more urban activities agglomerate in road segments with high accessibility, the more complicated thir impact on the thermal environment. However, the thermal environment is directly related to road construction, including factors such as road materials and road greening environments. In ArcGIS, the current spatial layout of the road network and the urban surface thermal environment parameters (including LST and the urban heat island (UHI) index) were overlaid to extract the LST of each road segment (natural discontinuity for classification) (Fig. 6-a), and the UHI index (Fig. 6-b).

Fig. 6-a shows that the LST of each road segment in the main urban area of Xuzhou exhibited considerable spatial variation over the years. In 1995, 2003, 2014 and 2019, the average LST of the road segment were 26.19 °C, 29.39 °C, 30.61 °C, and 30.02 °C, respectively, showing a clear warming trend. Among them, the thermal environment problems of the roads around the railway of the Xuzhou North Station, section of the East Third-ring Road, road segment of the northern industrial concentration area, and road segment of the commercial area west of Xuzhou Station were particularly prominent. The LSTs of the road segments along the bank of the Yunlong Lake and transit expressways were relatively low. This situation occurred because, in addition to the impact of road construction itself, high-temperature road segments were influenced by the surrounding land use properties. The railway areas at Xuzhou North Station, section of the East Third-ring Road, road segment of the northern industrial concentration area, and road segment of the commercial area west of Xuzhou Station are all agglomerations of urban activities, and the thermal environment of these areas is relatively high. Transit expressways and roads along the bank of Yunlong Lake were also affected by the surrounding land use. The transit expressway is surrounded by farmlands and woodlands, wiht only a section passing through urban built-up areas. The interweaving of the peripheral low temperature and road segment temperature reduced the thermal environment effect of the road segment to some extent.

UHIs were introduced and mapped to compare temperature data horizontally over the years (Fig. 6-b). The results showed that improvements in the urban road network and the influence of external transit traffic led to relatively small spatial variations in the urban road segment UHIs which were 0.57, 0.56, 0.56, and 0.55 for 1995, 2003, 2014, and 2019, respectively. This difference was relatively small, indicating that the role of roads in the urban thermal environment was relatively stable.

3.5. Thermal environmental effect of road structure

According to the measurement indices of road segment network centrality and road segment parameters over the past years—considering the values of road segment width, length and area data, the original data were processed using logarithms to eliminate the adverse effects caused by different index measurement units— road thermal environment parameters and road VCF were used as the basic data and anomalies were excluded from the correlation analysis.

The MGWR model was used to investigate the local heterogeneity pattern of the influencing factors of the urban road network structure on the thermal environment as they relate to location, thereby providing the basis for an in-depth analysis of the spatial pattern of the thermal environment differentiation of the urban road network.

In SPSS, the kurtosis and skewness values showed that the UHI_{index} data over the years met a normal distribution. Based on existing studies, the parameters of the road network structure, geometric characteristics of the road pavement, and road construction

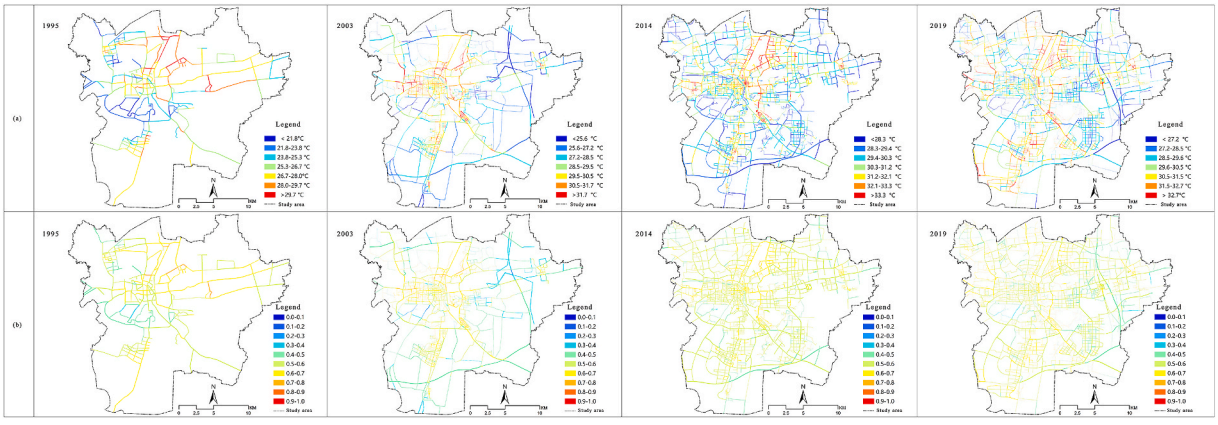

Fig. 6. Thermal environmental parameters of various road sections (a) LST; (b) UHI_{index}.

parameters were selected as influencing factors to analyze the thermal environment effect of the road network. The road network structure includes the three parameters of betweenness, closeness, and straightness; the geometric characteristics of the road surface include the road width and the length of the road segment; and the road construction parameters include the VCF of the road segment, with a total of six indicators as influencing factors. The statistical parameters of the means, standard deviations and sample sizes of the explanatory variables are presented in Table 3.

The descriptive statistics of the explanatory variables of road segments indicate that the road system gradually improved over the years, and the number of road segments increased from 282 in 1995–3174 in 2019. However, the length of road segments decreased yearly from an average of 1074.87 m/segment in 1995 to an average of 388.55 m/segment in 2019. Road connectivity is maintained at a relatively high level. The average VCF for roads first decreased and then increased, indicating a good trend for environmental construction related to the Xuzhou roads in recent years.

The above variables were subjected to a collinearity test using SPSS software. The VIF values were all below 7.5; thus, the indicators met the non-collinearity requirement and could be used in the regression analysis. In terms of the spatial distribution, the urban thermal environment has two forms: agglomeration and dispersion. In the study area, the degree of correlation between the attributes of the observation points in the adjacent space can be obtained through a spatial correlation analysis. Therefore, the spatial heterogeneity of urban road thermal environment can be explored using global or local spatial autocorrelation analyses.

3.5.1. Global autocorrelation analysis

ArcGIS software and the Moran index were used to analyze the surface thermal environment data for each road in the study area over the years (Table 4).

The global Moran index for 1995 was 0.391, the z-score was 1.491, and the P value was 0.136. These results suggest that the difference between the spatial and random patterns was not significant. Therefore, the 1995 data exhibited spatial randomness. In 2003, 2014, and 2019, the global Moran indices were 0.241, 0.385, and 0.394, respectively, the z-scores were 60.49, 100.73, and 18.77, respectively, and the P values were all 0.000, indicating that the data belonged to a clustering and not a spatial pattern; indicating that the spatial distribution of the surface thermal environment was generally positively correlated. In other words, the LST of the adjacent area is correlated; that is, the LST exhibits spatial aggregation, and the LST of each section transitions from disordered to ordered. Therefore, when performing GWR analysis on the road thermal environment, data from the three periods of 2003, 2014, and 2019 were chosen for comparative study.

Based on the results of the spatial correlation analysis, the OLS model suitable for spatial stationarity analysis for 1995 and the MGWR model suitable for spatial non-stationary analysis for 2003, 2014, and 2019 were selected.

3.5.2. Local autocorrelation analysis

The surface thermal environment data of the road pavements in the study area were analyzed using ArcGIS software. The local Moran index was calculated to detect four clusters: HH (high-high aggregation), LL (low-low aggregation), HL (high-low aggregation), and LH (low-high aggregation) (Fig. 7). In the spatial distribution of the thermal environment clustering in the main urban area of Xuzhou (Fig. 7), the uncolored area was insignificant. The figures indicate that the spatial aggregation of the LST of each road segment in the main urban area of Xuzhou over the years showed obvious spatial partitioning. In 1995, the hot clustering of road segment LST

Table 3
Descriptive statistics of explanatory variables of road sections over the years.

Year	Variables	Sample size	Average	Std dev	Unit
1995	Betweenness	282	0.04	0.04	
	Closeness	282	0.00	0.00	
	Straightness	282	0.86	0.03	
	width	282	71.98	19.70	m
	Length	282	1074.87	963.55	m
	VCF	282	0.38	0.27	
2003	Betweenness	1522	0.02	0.03	
	Closeness	1522	0.00	0.00	
	Straightness	1522	0.84	0.09	
	width	1522	29.31	19.19	m
	Length	1522	425.90	527.56	m
	VCF	1522	0.26	0.22	
2014	Betweenness	2403	0.01	0.03	
	Closeness	2403	0.00	0.00	
	Straightness	2403	0.84	0.05	
	width	2403	41.45	19.35	m
	Length	2403	408.55	406.65	m
	VCF	2403	0.31	0.18	
2019	Betweenness	3174	0.01	0.02	
	Closeness	3174	0.00	0.00	
	Straightness	3174	0.88	0.13	
	width	3174	28.84	18.52	m
	Length	3174	388.55	362.74	m
	VCF	3174	0.33	0.17	

Table 4
Global autocorrelation analysis of surface temperature of road sections in the study area.

Year	Distance Threshold	Moran's I	z	p
1995	1876.23	0.391	1.491	0.136
2003	2102.75	0.241	60.490	0.000
2014	1676.04	0.385	100.731	0.000
2019	1654.42	0.394	18.773	0.000

The data in Table 4 and the inverse square-distance method were used to calculate the space weights based on the fixed distance thresholds of 1876.23, 2102.75, 1676.04, and 1654.42, which were optimally selected over the years. The global Moran indices over the years were 0.391, 0.241, 0.385, and 0.394, respectively.

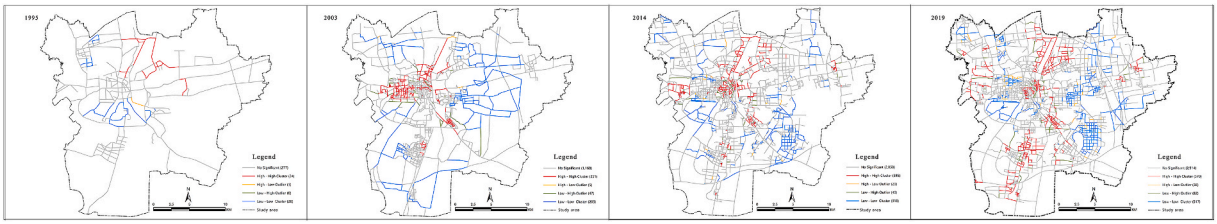

Fig. 7. Spatial cluster distribution of thermal environment on road sections in the main urban area of Xuzhou.

was mainly reflected around the Xuzhou North Station, whereas the cold cluster was distributed in Jiuli Lake, Yunlong Lake and the surrounding areas of Yunlong Mountain. In 2003, the scale of cold and hot clusters expanded, with the hot clusters mainly distributed on the west side and southward area of Xuzhou North Station, the residential area from the northern bank of Yunlong Lake to the west second ring of the north second ring road, and the commercial service facilities area in the southwestern part of Daguozhuang Airport. The cold clusters were located in the surrounding areas. In 2014, the hot cluster area expanded near Xuzhou North Station, shrank on the north bank of Yunlong Lake, and relocated to the vicinity of Xuzhou Station, whereas it remained unchanged in the area of commercial service facilities southwest of Daguozhuang Airport. Simultaneously, cold clusters began to appear in Xuzhou New District. In 2019, the hot and cold clusters presented relatively distinct partitions. The Xuzhou North Station, Tongshan District in the south, and the southwest commercial service facility area of Daguozhuang Airport formed a hot cluster area that ran through the main urban area. The cold cluster intensified and expanded northward, forming an overall cold cluster area to the east. Cold clusters remained along the banks of Yunlong Lake. The anomalous clustering data of HL and LH over the years were clearly interspersed and distributed as independent small areas, and their numbers were relatively small.

3.5.3. Spatial stationarity analysis

A global autocorrelation analysis of road and thermal environments conducted in 1995 showed that the data exhibited spatial randomness. Therefore, the OLS model was used for the regression analysis. A significance test, collinearity diagnosis, and normality test of the residuals were used to validate the explanatory power of the OLS model. First, an OLS regression model was constructed using the descriptive statistics of the model factors. Then, an OLS regression analysis was performed using SPSS (Table 5).

Based on the analysis results, the expression for the OLS regression model of the road thermal environment in the study area is as follows:

UHI_{index} = 0.610–0.333*betweenness-1194.5*closeness+0.197*straightness-8.898*10-6*road width+1.012*10-7*road length-0.160*VCF

The regression coefficient is positive, indicating that the explanatory variable has a positive effect on the explained variable, and

Table 5
Parameter estimation of the OLS model between UHI_{index} and road heat effect factors in 1995.

	Non-standardized coefficient		t	Significance
	B	Std dev		
Intercept	0.610	0.113	5.378	0.000
Betweenness	−0.333	0.092	−3.620	0.000
Closeness	−1194.500	196.499	−6.079	0.000
Straightness	0.197	0.130	1.518	0.130
Width	−8.898E-6	0.000	−0.050	0.960
Length	1.012E-7	0.000	0.030	0.976
VCF	−0.160	0.016	−9.837	0.000

dependent variables:UHI_{index}.

vice versa. The regression coefficients of betweenness, closeness, and VCF were −033, −1194.5, and −0.160, respectively, and the P values were all <0.05, indicating that they all have a significant negative correlation with road temperature. The P values of the straightness, road width, and road segment length were all >0.05, indicating that their relationship with the road thermal environment was not sufficiently significant.

Next, we analyzed the results of the OLS model, including the significance and OLS model tests, multicollinearity analysis, and residual distribution test. In SPSS, the significance test of the OLS model and the test of the OLS model of the road segment LST and traffic network factors showed the following.

In the OLS regression model, the F value was 22.673, the p value was 0.000 (<0.05), and the linear relationships among the variables were evident. The R^2 value was 0.331, indicating that approximately one-third of the variation in the dependent variable could be explained by these results. The actual number of variables was considered, and the adjusted R^2 value was 0.316; that is, 31.6 % of the variation in the independent variables could be explained, indicating that the fit was not ideal. This result occurred mainly due to data limitations; relatively few urban road factors were selected to participate in the thermal environment, and the variable influences of special factors, such as the land use nature of the surrounding areas, were not considered. In this study, the results of linear regression were used to analyze the degree of effect rather than to predict LST; therefore, the requirement for R^2 could be appropriately reduced.

By analyzing multicollinearity, the VIF values of betweenness, closeness, straightness, road width, road segment length, and VCF were found to be 1.232, 2.037, 1.379, 1.239, 1.087, and 1.941, respectively. The VIF values of the variables ranged from 1.087 to 2.037, all of which were <7.5. The assumption of collinear variables was overturned, indicating that there was no significant correlation among the independent variables and that all indicators satisfied the analysis conditions. The residuals met the requirements of the linear model, and the normality test was passed.

3.5.4. Spatial nonstationary GWR analysis

This study used an MGWR model to calculate the spatial differentiation of road segments and independent variable factors during 2003, 2014, and 2019.

First, a stationarity test of the model space was performed. Table 6 shows the fitting results of the OLS, classic GWR and MGWR models for the three periods (2003, 2014, and 2019). Three indicators—AICc, adjusted R^2,and RSS—were selected to evaluate the performance of each regression model. The larger the R^2, the smaller the AICc and RSS values, indicating a better performance of the model [50]. According to the fitting results from the AICc and adjusted R^2 values, the GWR and MGWR models were both better than the OLS model in reflecting the non-stationary spatial relationship of the thermal environment. When the global variables did not have a spatial non-stationary relationship, the MGWR model performed the best. Based on a comprehensive comparison of the data for the three periods, the thermal environment of the road segment in 2014 was selected for analysis.

A regression coefficient analysis was then performed, including the global and local analysis stages. The MGWR model was first analyzed in the global analysis stage (Table 7). As shown, the two variables of betweenness and closeness in the road network centrality parameters did not have a significant linear impact on the LST of the road segment, whereas the length and straightness of the road segment had a significant negative impact. Straightness refers to the efficiency of access to the urban road transportation network. The higher the straightness, the higher the road traffic efficiency and the fewer the agglomerated urban activities. Similarly, the longer the road segment, the more traffic activity is retained and the introduction of other urban activities is reduced; however, this situation will not cause an increase in temperature. Road VCF also had a significant negative effect on the LST of the road segment. Greening is generally acknowledged to reduce road LST effectively. Additionally, road width has a positive effect on the thermal environment, the wider the road width, the larger the area of the vehicular road surface that receives solar radiation, and the higher the temperature increase.

Based on the approximate *t*-test [50], when the coefficient of the thermal environment influence index of the road segment $|t| < 1.96$ and $p > 0.05$, there was no significant effect, indicating that the interpretability of this indicator on the LST in the road segment was very weak. Based on the local spatial analysis of the effect of the road network on the thermal environment and considering that the focus here was the analysis of the road network structure effect on the thermal environment, the distribution pattern of the road segment effect on the LST was explored spatially. From the perspective of space stationarity, road betweenness and closeness had space

Table 6
Comparison of global OLS regression and GWR fitting results (statistical data).

Model parameter		AICC	R^2	Adjust-R^2	RSS	Enp
2003	OLS	3064.530	0.566	0.564	660.381	–
	GWR	2306.681	0.848	0.805	231.360	332.408
	MGWR	2103.675	0.862	0.826	210.557	313.969
2014	OLS	5512.991	0.423	0.422	1385.927	–
	GWR	4143.970	0.818	0.765	436.385	548.012
	MGWR	3696.533	0.829	0.789	411.154	452.849
2019	OLS	8067.335	0.260	0.259	2348.446	–
	GWR	5968.269	0.767	0.709	738.619	634.058
	MGWR	5522.923	0.783	0.736	688.713	560.582

RSS: residual sum of squares.
Enp: Effective number of parameters (trace(S)).

Table 7
Global regression coefficients of MGWR model.

Variable	Est.	SE	t (Est/SE)	p-value
Intercept	0.000	0.016	0.000	1.000
Betweenness	0.021	0.023	0.912	0.362
Closeness	0.024	0.023	1.081	0.280
Straightness***	−0.073	0.016	−4.560	0.000
Width***	0.067	0.016	4.059	0.000
Length***	−0.056	0.017	−3.345	0.001
VCF***	−0.634	0.017	−38.061	0.000

stationarity, whereas straightness, length, VCF, and width had space non-stationarity. A key t value of 1.960 (corresponding to the upper limit of the 95 % confidence level of the *t*-test) and P value < 0.05 were selected as the boundaries. After performing an approximate *t*-test, the correlation coefficient of each influencing factor in the regional space was retained, and the spatial distribution of the local regression coefficients of each influencing factor was plotted (Fig. 8), visually showing the pattern of the significance of each influencing factor on the road surface thermal environment as it relates to location.

As shown in Fig. 8, the length, width, and road connectivity effects of the road segment on its surface thermal environment showed significant spatial differentiation, and the length effect of the road segment was most evident in the old urban area on the northern bank of Yunlong Lake. The VCF showed a clear negative effect on the global thermal environment.

Subsequently, a local analysis was performed. Statistical descriptions of the local variables used in the MGWR model are presented in Table 8. A comparative analysis of the results showed that the positive and negative values of the regression coefficient of each variable reflected different directionalities, indicating that there were two types of effects—positive and negative— on the thermal environment. Concurrently, these variables had notably the same effect on the sample points of most road segments in the study area. The mean and median values of straightness, length, and VCF were negative, whereas those of width were positive, indicating their positive and negative effects on the thermal environment of the road segments.

4. Discussion

4.1. Roads: the temperature change trend and city designation as a heat island or cold island

The urban road ontology is a typical impermeable surface and manifestation of urbanization in physical spaces [51]. Urban roads are high heat storage bodies in the urban thermal environment that increase the thermal conductivity of the underlying surfaces in the city, and thus are important space carriers of the UHI effect [52,53].

Here, we analyzed the thermal environment based on urban road segments. The results show that in the overall urban thermal environment—judging from the road UHIs over the years—the average UHI_{index} was ~0.56, which is in the medium-temperature region as a whole, indicating that the urban road temperature is higher than the urban average temperature and has stability. Considering the network characteristics of urban roads [54] and the connectivity function of a series of functional areas [55,56], the road network has a reinforcing effect on connecting UHI patches, improving the overall connectivity of heat islands, and forming a heat island aggregation area [57]. Urban roads have a clear positive effect on promoting the UHI effect. Simultaneously, in the context of splitting the connectivity of thermal environment areas for zonal control of the thermal environment [58–60], improvements in the road thermal environment can block the connection and aggregation of each heat island functional area.

Roads in cities are constantly improving. We consider urban roads—the carriers of the urban skeleton structure—as a primary element in the urban morphological structure and quantify the structure and LST of urban roads in different periods based on individual road segments. This process shows that improvements in the main structure of the urban road network lead to obvious non-stationarity in the thermal environment of the roads; that is, the factors affecting the urban road temperature vary spatially.

4.2. Spatial differentiation of the road thermal environment: individual influencing factors

Roads, by themselves, are impervious [61]. Existing studies have shown that the geometric characteristics, material composition, structural characteristics, green coverage, and construction of the surrounding functional areas of road segments are all important

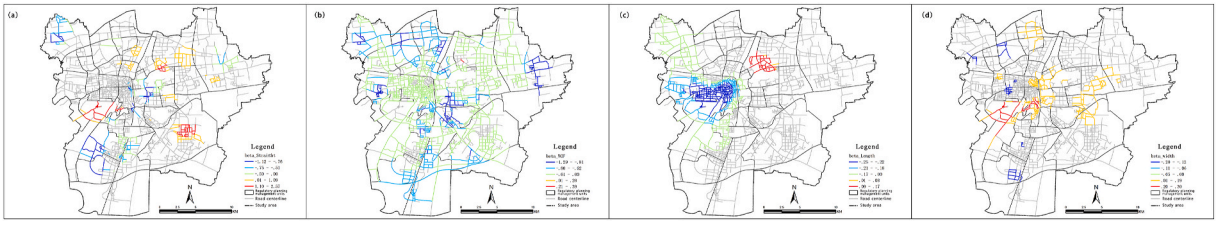

Fig. 8. The coefficient of influence of significant influencing variables on LST of the road (a) Straight; (b) VCF; (c) Length; (d) Width.

Table 8
Descriptive statistics of regression coefficients of the MGWR model of road LST.

variables	Average	Std dev	Minimum	Median	Maximun
Intercept	−0.138	0.355	−1.139	−0.151	0.827
Straightness	−0.037	0.485	−1.116	−0.119	2.574
Width	0.021	0.089	−0.202	0.033	0.298
Length	−0.094	0.1	−0.246	−0.056	0.168
VCF	−0.473	0.233	−1.286	−0.448	0.389

factors affecting the thermal environment of the road itself [62–65]. Urban structure affects the thermal environment [66,67]. and since a road is a skeleton for urban structures [68] it also has an impact. Here, we selected the index factors of the structural, geometric, and self-construction attributes of road segments. We found that the self-organizing structural characteristics of road segments are also important factors affecting the thermal environment. In particular, straightness—a structural indicator of roads—and road segment length in urban road organizations showed a significant overall negative correlation with the road thermal environment. In general, higher road straightness indicates higher traffic efficiency of the urban road traffic network, and thus stronger traffic attributes; fewer urban residential activities are associated with such road structures. The lower the frequency of interaction between the urban functional area and the road, the less the thermal environmental attributes of the road overlay thermal emissions from urban activities. Therefore, thermal emissions are close to those of the impervious surface itself. For high-grade roads with greater straightness, the focus of thermal environment regulations should be on the road construction level, considering factors such as increasing road greening and changing road pavement materials.

In China's urban road network organization, the road segments in the old urban area are shorter than those in the new urban areas, and the length of the low-grade roads is shorter than that of the high-grade roads. The shorter the road segments, the stronger the lifestyle attributes of the roads and the more their thermal environments are influenced by the surrounding thermal environment. In other words, the greater the superposition of heat emissions from surrounding urban functional areas, the more likely that the thermal environment will contain a high number of urban functional attributes because of the impermeable surface itself. Similarly, in urban road networks in China, roads in old urban areas are often narrower than those in new urban areas. The width of low-grade roads is narrower than that of high-grade roads; the narrower the road width, the stronger the lifestyle attributes of the roads and the wider the width, the stronger the traffic attributes of the road. The thermal environment of narrow roads is affected more by the surrounding thermal environment; that is, the superposition of heat emissions from the functional areas of the surrounding cities is greater. Therefore, based on the thermal environment attributes of the impermeable surface, the thermal environment of narrow roads contains more urban functional attributes—wide roads mostly reflect the thermal environmental attributes of their impervious surfaces.

Green cover has a negative effect on the thermal environment, and greening enhancement is an effective measure for reducing road LST [69,70]. However, in urban road spaces, the regulation of the thermal environment by improving greenery shows obvious spatial non-stationarity. Therefore, thermal environment improvements based on the global scale of greening construction cannot reflect significant space efficiency/benefit. Thus, greening improvements in strongly correlated areas should be emphasized. At a later stage, studies related to greening belt width, plant combinations, and seasonal (season and time) changes could be considered to optimize the thermal environment.

4.3. Guidance for space planning

This study validated the influence of the self-organizing spatial structure characteristics of urban roads on LST and proposed a strategy for improving LST aimed at the structural, geometric, and self-construction attributes of roads. Owing to the constant development and changes in urban roads, methods of urban traffic organization—subways, light rail, and sky rail— are becoming increasingly diverse, and the construction orientation of urban road structures—such as policies on narrow roads and dense road networks—is changing [71]. During road optimization and adjustment, the same road segment characteristics are located in different areas and have different structural attributes; thus, there are large differences in their thermal environments. As such, we introduced a GWR analysis to explore the main factors influencing road LST in different spatial regions and analyzed targeted measures that can improve this. Based on the study results, we believe that, in addition to improving construction characteristics of the road segment itself, the thermal environment of urban roads should be guided by the optimization of the road structure from the perspective of the overall structure of urban roads, based on the planning system of each region or country.

The network structure and road segment construction of urban roads are important factors affecting the urban thermal environment. When the urban form was relatively simple in the early stages, the impact of the urban network structure on the thermal environment was relatively insignificant. With the expansion of the urban form, complexity of the internal structure, and the improvement of road system construction, the influence of the urban road network structure on the thermal environment has also gradually increased. The road thermal environment reflects clear spatial non-stationarity. Under China's urban-rural planning system, the structural optimization of the road system should be guided by the overall planning and scientific organization of the road network and supplemented by optimizing the layout of various land use functional areas. In lower-level planning, detailed regulatory planning management units should be emphasized as the boundary of the space partition. Based on the performance of the thermal environment effect of roads in different regions, a construction orientation for each region should be proposed, and the management and control of various construction indicators should be clarified. Road cross-sectional structures and greening configurations should be optimized

segment-by-segment and implemented in the constructive detailed planning stage.

4.4. Study limitations and future directions

First, this study emphasized the influence of urban road structures on LST, which is only limited to two-dimensional spatial scales to carry out the correlation study, and does not investigate in any depth the three-dimensional spatial scales of the construction of road sections and other internal constructions. Different levels of urban roads have different arrangements of paving materials, plant and green configurations, cross-sectional forms, and spatial layouts of surrounding buildings [72], resulting in different albedos, plant cooling effects, and spatial morphologies, which also have an impact on the LST of urban roads. Therefore, thermal environment mechanisms of different road attributes and surrounding building spaces should be explored in a refined, three-dimensional, and comprehensive manner in future studies. Second, LST is time dependent [73], and the retrieved LST data used here had high spatial resolution. Dynamic changes in the environment and each component of urban roads exert different thermal environmental performances at different time points. This study employed commonly used data types to explore more accurate methods of dynamically and continuously quantifying the all-weather and all-seasonal phases of roads. Even LST within the full life cycle is a key consideration for future research. Finally, although this study selected typical cities of an average size in China as the research object, the road network of each city is unique. For example, urban transportation modes differ under different climatic and geographical conditions. In future, thermal environmental effects of urban roads should be systematically classified and explored.

5. Conclusion

Taking the main urban area of Xuzhou City as the study area, this study clarified the influence of road structure on LST through multi-period data analysis, and further explored the effects of urban roads on the LST of road segments at the structural, geometric, and their own construction attribute levels. The following conclusions were obtained: (1) the contribution of road land to the UHI effect is relatively stable, and the overall temperature is in the intermediate temperature range. Based on the network structure characteristics of roads, connected UHI patches had a greater promotional effect on LST. From the perspective of segmenting UHI patches for individual management, roads provide an important opportunity to improve the overall urban thermal structure. (2) Based on a quantitative study of the factors, the self-organizing structural characteristics of roads are important factors affecting their thermal environment, especially the straightness factor, which shows a significant overall negative correlation with the road thermal environment. Concurrently, the road segments length and width have a significant overall negative and positive correlation with the road thermal environment, respectively. Among the self-construction attributes, VCF has a negative effect on the thermal environment, but reflects an obvious spatial non-stationary relationship.

In summary, this study enriches research perspectives on the relationship between urban spatial structures and LST as well as research levels of the relationship between roads and LST, quantitatively explores the influence of self-organizing characteristics of urban road structures on LST, explains the differences in the influence of various factors of urban road structures on LST, and clarifies the importance of proposing differentiated and targeted strategies for different regions. Urban roads form the skeleton of urban structures. This quantitative exploration of the thermal environment effect of urban roads can provide ideas for urban planners and administrators when formulating policies to address the organization and morphological development of urban traffic associated with the urban thermal environment. The method proposed here can be applied to other countries and cities with different climatic environments and morphological types to better guide and regulate urban thermal environments and synergic construction of urban spatial structures.

Funging

Anhui Philosophy and Social Science Planning Youth Project (AHSKQ2022D153); Talent Project of Anhui Science and Technology University (Xinbin Liang JZWD202201,230057); Research and Development Fund Project of Anhui Science and Technology University (811499); Natural Science Key Research Project of Anhui Education Department (KJ2020A0078); the Training Program of Innovation and Entrepreneurship for Undergraduates of Anhui Province (S202210879018, S202310879142); the National Training Program of Innovation and Entrepreneurship for Undergraduates (202310879073).

Ethics declarations

Review and/or approval by an ethics committee was not needed for this study because the study do not include human or animal participation.

Data availability statement

The data supporting the findings of this study are available on request from the corresponding author. The data are not publicly available due to privacy and ethical restrictions.

CRediT authorship contribution statement

Nana Guo: Writing – original draft, Software, Methodology, Funding acquisition, Formal analysis, Data curation, Conceptualization. **Xinbin Liang:** Writing – original draft, Visualization, Validation, Supervision, Project administration, Funding acquisition. **Lingran Meng:** Writing – review & editing, Writing – original draft, Methodology, Formal analysis, Data curation.

Declaration of competing interest

The authors declare that they have no known competing financial interests or personal relationships that could have appeared to influence the work reported in this paper.

Acknowledgements

The authors acknowledge support from the Anhui Philosophy and Social Science Planning Youth Project (AHSKQ2022D153); Talent Project of Anhui Science and Technology University (Xinbin Liang JZWD202201,230057); Research and Development Fund Project of Anhui Science and Technology University (811499); Natural Science Key Research Project of Anhui Education Department (KJ2020A0078); the Training Program of Innovation and Entrepreneurship for Undergraduates of Anhui Province (S202210879018, S202310879142); the National Training Program of Innovation and Entrepreneurship for Undergraduates (202310879073) as well as data support from the China Meteorological Administration, the Chinese Academy of Sciences Computer Network Information Center and the Xuzhou urban planning bureau, and Shuaixiang Jia, Xinyi Liu, Wenjie Li, Chen Ye, Huiqi Li and Yuecen Liu whose majors are in urban and rural planning, College of Architecture, Anhui Science and Technology University. We also thank the editors and the anonymous reviewers for their helpful suggestions in various stages.

References

[1] G. Zhou, C. Li, Y. Liu, J. Zhang, Complexity of functional urban spaces evolution in different aspects: based on urban land use conversion, Complexity 2020 (2020) 1–12, https://doi.org/10.1155/2020/9741203.
[2] S. Lei, L. Zhe, Y. Zhiwu, L. Zhuohan, Evaluation and research of site selection based on performance of urban spatial structures, in: 2014 Fifth International Conference on Intelligent Systems Design and Engineering Applications (ISDEA), IEEE, 5th International Conference on Intelligent Systems Design and Engineering Applications (ISDEA), 2014, pp. 451–453.
[3] P. Xiao, Evaluation of urban residence, employment and transportation mode in beijing, in: L.C. Dong, P.H. Huang, T. Ozbakkaloglu (Eds.), PROCEEDINGS of the 2016 INTERNATIONAL CONFERENCE on ARCHITECTURAL ENGINEERING and CIVIL ENGINEERING, Vol. 72, International Conference on Architectural Engineering and Civil Engineering (AECE), 2016, pp. 331–335.
[4] P. Coseo, L. Larsen, Accurate characterization of land cover in urban environments: determining the importance of including obscured impervious surfaces in urban heat island models, Atmosphere 10 (2019) 347, https://doi.org/10.3390/atmos10060347.
[5] Y. Rui, Y. Ban, Exploring the relationship between street centrality and land use in Stockholm, Int. J. Geogr. Inf. Sci. 28 (2014) 1425–1438, https://doi.org/10.1080/13658816.2014.893347.
[6] E. Mirabi, P.J. Davies, A systematic review investigating linear infrastructure effects on Urban Heat Island (UHIULI) and its interaction with UHI typologies, Urban Clim. 45 (2022) 101261, https://doi.org/10.1016/j.uclim.2022.101261.
[7] M. Moghbel, A.A. Shamsipour, Spatiotemporal characteristics of urban land surface temperature and UHI formation: a case study of Tehran, Iran, Theor. Appl. Climatol. 137 (2019) 2463–2476, https://doi.org/10.1007/s00704-018-2735-7.
[8] A. Piracha, M.T. Chaudhary, Urban air pollution, urban heat island and human health: a review of the literature, Sustainability 14 (2022) 9234, https://doi.org/10.3390/su14159234.
[9] V.R.S. Cheela, M. John, W. Biswas, P. Sarker, Combating urban heat island effect—a review of reflective pavements and tree shading strategies, BUILDINGS-BASEL 11 (2021) 93, https://doi.org/10.3390/buildings11030093.
[10] C. Yang, J. Siao, W. Yeh, Y. Wang, A study on heat storage and dissipation efficiency at permeable road pavements, Materials 14 (2021) 3431, https://doi.org/10.3390/ma14123431.
[11] E. Husni, G.A. Prayoga, J.D. Tamba, Y. Retnowati, F.I. Fauzandi, R. Yusuf, B.N. Yahya, Microclimate investigation of vehicular traffic on the urban heat island through IoT-Based device, Heliyon 8 (2022) e11739, https://doi.org/10.1016/j.heliyon.2022.e11739.
[12] J. Wu, S. Li, N. Shen, Y. Zhao, H. Cui, Construction of cooling corridors with multiscenarios on urban scale: a case study of shenzhen, Sustainability 12 (2020) 5903, https://doi.org/10.3390/su12155903.
[13] Y.S. Ünal, C.Y. Sonuç, S. Incecik, H.S. Topcu, D.H. Diren-Üstün, H.P. Temizöz, Investigating urban heat island intensity in Istanbul, Theor. Appl. Climatol. 139 (2020) 175–190, https://doi.org/10.1007/s00704-019-02953-2.
[14] C. Yang, J. Siao, W. Yeh, Y. Wang, A study on heat storage and dissipation efficiency at permeable road pavements, Materials 14 (2021) 3431, https://doi.org/10.3390/ma14123431.
[15] X. Zhang, H. Li, N. Xie, M. Jia, B. Yang, S. Li, Laboratorial investigation on optical and thermal properties of thermochromic pavement coatings for dynamic thermoregulation and urban heat island mitigation, Sust. Cities Soc. 83 (2022) 103950, https://doi.org/10.1016/j.scs.2022.103950.
[16] Y. Lu, M.A. Rahman, N.W. Moore, A.J. Golrokh, Lab-controlled experimental evaluation of heat-reflective coatings by increasing surface albedo for cool pavements in urban areas, Coatings 12 (2022) 7, https://doi.org/10.3390/coatings12010007.
[17] C. Xi, C. Ren, R. Zhang, J. Wang, Z. Feng, F. Haghighat, S. Cao, Nature-based solution for urban traffic heat mitigation facing carbon neutrality: sustainable design of roadside green belts, Appl. Energy 343 (2023) 121197, https://doi.org/10.1016/j.apenergy.2023.121197.
[18] R.R. Shaker, Y. Altman, C. Deng, E. Vaz, K.W. Forsythe, Investigating urban heat island through spatial analysis of New York City streetscapes, J. Clean. Prod. 233 (2019) 972–992, https://doi.org/10.1016/j.jclepro.2019.05.389.
[19] C. Xi, C. Ren, R. Zhang, J. Wang, Z. Feng, F. Haghighat, S. Cao, Nature-based solution for urban traffic heat mitigation facing carbon neutrality: sustainable design of roadside green belts, Appl. Energy 343 (2023) 121197, https://doi.org/10.1016/j.apenergy.2023.121197.
[20] G. Del Serrone, P. Peluso, L. Moretti, Evaluation of microclimate benefits due to cool pavements and green infrastructures on urban heat islands, Atmosphere 13 (2022) 1586, https://doi.org/10.3390/atmos13101586.
[21] Y. Wang, Q. Zhan, W. Ouyang, How to quantify the relationship between spatial distribution of urban waterbodies and land surface temperature? Sci. Total Environ. 671 (2019) 1–9, https://doi.org/10.1016/j.scitotenv.2019.03.377.
[22] J. Lin, Y. Ban, Comparative analysis on topological structures of urban street networks, ISPRS Int. J. Geo-Inf. 6 (2017) 295, https://doi.org/10.3390/ijgi6100295.

[23] S. Porta, E. Strano, V. Iacoviello, R. Messora, V. Latora, A. Cardillo, F. Wang, S. Scellato, Street centrality and densities of retail and services in bologna, Italy, Environ. Plann. Plann. Des. 36 (2009) 450–465, https://doi.org/10.1068/b34098.

[24] L. Yongqiang, Z. Xinqi, Z. Lin, Relationships between street centrality and spatial distribution of functional urban land use:Acase study of Beijing central city, Geogr. Res. 36 (2017) 1353–1363.

[25] E. Strano, M. Viana, L. Da Fontoura Costa, A. Cardillo, S. Porta, V. Latora, Urban street networks, a comparative analysis of ten European cities, Environ. Plann. Plann. Des. 40 (2013) 1071–1086, https://doi.org/10.1068/b38216.

[26] X. Xu, H. Pei, C. Wang, Q. Xu, H. Xie, Y. Jin, Y. Feng, X. Tong, C. Xiao, Long-term analysis of the urban heat island effect using multisource Landsat images considering inter-class differences in land surface temperature products, Sci. Total Environ. 858 (2023) 159777, https://doi.org/10.1016/j.scitotenv.2022.159777.

[27] X. Zhang, K. Wang, Y. Song, Comparison of urban heat island retrieval method from Landsat TM thermal data, in: W. Ju, S. Zhao (Eds.), GEOINFORMATICS 2007: REMOTELY SENSED DATA AND INFORMATION, PTS 1 AND 2, vol. 6752, SPIE, Bellingham, Wash, 2007, p. 67522A.

[28] L. Yang, K. Yu, J. Ai, Y. Liu, W. Yang, J. Liu, Dominant factors and spatial heterogeneity of land surface temperatures in urban areas: a case study in fuzhou, China, Remote Sens 14 (2022) 1266, https://doi.org/10.3390/rs14051266.

[29] A. Kashki, M. Karami, R. Zandi, Z. Roki, Evaluation of the effect of geographical parameters on the formation of the land surface temperature by applying OLS and GWR, A case study Shiraz City, Iran, Urban Clim. 37 (2021) 100832, https://doi.org/10.1016/j.uclim.2021.100832.

[30] H. Zhao, Z. Ren, J. Tan, The spatial patterns of land surface temperature and its impact factors: spatial non-stationarity and scale effects based on a geographically-weighted regression model, Sustainability 10 (2018) 2242, https://doi.org/10.3390/su10072242.

[31] X. Liang, X. Ji, N. Guo, L. Meng, Assessment of urban heat islands for land use based on urban planning: a case study in the main urban area of Xuzhou City, China, Environ. Earth Sci. 80 (2021), https://doi.org/10.1007/s12665-021-09588-5.

[32] G. Del Serrone, P. Peluso, L. Moretti, Evaluation of microclimate benefits due to cool pavements and green infrastructures on urban heat islands, Atmosphere 13 (2022) 1586, https://doi.org/10.3390/atmos13101586.

[33] V.R.S. Cheela, M. John, W. Biswas, P. Sarker, Combating urban heat island effect—a review of reflective pavements and tree shading strategies, BUILDINGS-BASEL 11 (2021) 93, https://doi.org/10.3390/buildings11030093.

[34] Y. Wang, J. Zhang, S. Tong, E. Guo, Monitoring the trends of aeolian desertified lands based on time-series remote sensing data in the Horqin Sandy Land, China, Catena 157 (2017) 286–298, https://doi.org/10.1016/j.catena.2017.05.030.

[35] X.M. Jin, R.H. Guo, Q. Zhang, Y.X. Zhou, D.R. Zhang, Z. Yang, Response of vegetation pattern to different landform and water-table depth in Hailiutu River basin, Northwestern China, Environ. Earth Sci. 71 (2014) 4889–4898, https://doi.org/10.1007/s12665-013-2882-1.

[36] B.C. Rundquist, The influence of canopy green vegetation fraction on spectral measurements over native tallgrass prairie, Remote Sens. Environ. 81 (2002) 129–135, https://doi.org/10.1016/S0034-4257(01)00339-X.

[37] Y. Jia, X. Qi, R. Huang, Y. Zhou, Spatiotemporal variation and driving factors of vegetation coverage in Shanxi Province, China, J. Appl. Ecol. 35 (2024) 1073–1082, https://doi.org/10.13287/j.1001-9332.202403.023.

[38] K.D. Y., Y. Q., F.L. C., Monitoring and predicting the changes of vegetation coverage in Shijiazhuang from 1995 to 2015, in: 2016 IEEE International Geoscience and Remote Sensing Symposium, IGARSS), 2016, pp. 2324–2327.

[39] Sergio Porta, Emanuele Strano, Valentino Lacoviello, Roberto Messora, Vito Latora, Street centrality and densities of retail and services in Bologna, Italy, Environ. Plann. 36 (3) (2009) 450–465.

[40] M. Roosta, M. Javadpoor, M. Ebadi, A study on street network resilience in urban areas by urban network analysis: comparative study of old, new and middle fabrics in shiraz, Int. J. Urban Sci. 26 (2022) 309–331, https://doi.org/10.1080/12265934.2021.1911676.

[41] S. Boccaletti, V. Latora, Y. Moreno, M. Chavez, D.U. Hwang, Complex networks: structure and dynamics, Complex Systems and Complexity Science 424 (2006) 175–308.

[42] Y. Chao-Hui, L. Yan-Fang, W. Xiao-Jian, Study on the multi-scale relationship between road network CENTERALITY and social economic activities distribution in wuhan, Hum. Geogr. 32 (2017) 104–112.

[43] S. Andres, M. Michael, Urban network analysis. A new toolbox for ArcGIS, Rev. Int. Géomatique 22 (2012).

[44] F. Yang, L. Zhai, Q. Qiao, Y. Zhu, Y. Zhen, Analysis of spatial structure characteristics of urban roads based on network-centrality measure, Science of Surveying and Mapping 44 (2019) 127–134.

[45] X. Zhu, C. Huang, B. Wu, H. Su, W. Jiao, L. Zhang, Research on remote sensing drought monitoring by considering spatial non-stationary characteristics, Journal of Remote Sensing 23 (2019) 487–500.

[46] S. Yin, J. Liu, Z. Han, Relationship between urban morphology and land surface temperature—a case study of Nanjing City, PLoS One 17 (2022) e260205, https://doi.org/10.1371/journal.pone.0260205.

[47] B. Lu, Y. Ge, K. Qin, J. Zheng, A review on geographically weighted regression, Geomatics Inf. Sci. Wuhan Univ. 45 (2020) 1356–1366, https://doi.org/10.13203/j.whugis20190346.

[48] C. Fang, H. Liu, G. Li, D. Sun, Z. Miao, Estimating the impact of urbanization on air quality in China using spatial regression models, Sustainability 7 (2015) 15570–15592, https://doi.org/10.3390/su71115570.

[49] C. Chen, C. Xiu, L. Cheng, Matching score of disaster prevention green space-street network-population in large city based on multiple centrality analysis model: a case study of shenyang, Journal of Catastrophology 31 (2016) 219–225.

[50] J. Liu, L. Shen, Y. Huang, H. Wang, Comparison of the relationships between urban form and intensity of heat island during the day and night:A case study of beijing, Geomatics World 27 (2020) 23–31, https://doi.org/10.3969/j.issn.1672-1586.2020.05.005.

[51] A. Dwivedi, M.V. Khire, Application of split- window algorithm to study Urban Heat Island effect in Mumbai through land surface temperature approach, Sust. Cities Soc. 41 (2018) 865–877, https://doi.org/10.1016/j.scs.2018.02.030.

[52] A.K. Chandrappa, K.P. Biligiri, Development of pavement-surface temperature predictive models: parametric approach, J. Mater. Civ. Eng. 28 (2016), https://doi.org/10.1061/(ASCE)MT.1943-5533.0001415.

[53] A. Tzavali, J.P. Paravantis, G. Mihalakakou, A. Fotiadi, E. Stigka, Urban heat island intensity: a literature review, Fresenius Environ. Bull. 24 (2015) 4535–4554.

[54] Z. Tian, L. Jia, H. Dong, F. Su, Z. Zhang, Analysis of urban road traffic network based on complex network, Procedia Eng. 137 (2016) 537–546, https://doi.org/10.1016/j.proeng.2016.01.290.

[55] J. Shim, J. Yeo, An evaluation method of road link functionality using individual trajectory data and weighted network analysis, J. Adv. Transp. 2022 (2022) 1–10, https://doi.org/10.1155/2022/4960882.

[56] V.R.S. Cheela, M. John, W. Biswas, P. Sarker, Combating urban heat island effect—a review of reflective pavements and tree shading strategies, BUILDINGS-BASEL 11 (2021) 93, https://doi.org/10.3390/buildings11030093.

[57] J. Tang, L. Di, J. Xiao, D. Lu, Y. Zhou, Impacts of land use and socioeconomic patterns on urban heat Island, Int. J. Remote Sens. 38 (2017) 3445–3465, https://doi.org/10.1080/01431161.2017.1295485.

[58] A. Gioia, L. Paolini, A. Malizia, R. Oltra-Carrió, J.A. Sobrino, Size matters: vegetation patch size and surface temperature relationship in foothills cities of northwestern Argentina, Urban Ecosyst. 17 (2014) 1161–1174, https://doi.org/10.1007/s11252-014-0372-1.

[59] Z. Yu, J. Zhang, G. Yang, J. Schlaberg, Reverse thinking: a new method from the graph perspective for evaluating and mitigating regional surface heat islands, Remote Sens 13 (2021) 1127, https://doi.org/10.3390/rs13061127.

[60] J. Jiang, Y. Zhou, X. Guo, T. Qu, Calculation and expression of the urban heat island indices based on GeoSOT grid, Sustainability 14 (2022) 2588, https://doi.org/10.3390/su14052588.

[61] A. Feinberg, Urbanization heat flux modeling confirms it is a likely cause of significant global warming: urbanization mitigation requirements, Land 12 (2023) 1222, https://doi.org/10.3390/land12061222.

[62] R.R. Shaker, Y. Altman, C. Deng, E. Vaz, K.W. Forsythe, Investigating urban heat island through spatial analysis of New York City streetscapes, J. Clean. Prod. 233 (2019) 972–992, https://doi.org/10.1016/j.jclepro.2019.05.389.

[63] O. Gervasi, B. Murgante, S. Misra, C. Garau, I. Blečić, D. Taniar, B.O. Apduhan, A.M.A.C. Rocha, E. Tarantino, C.M. Torre, Empirical evaluation of urban heat island pavements related. Cagliari case study, in: O. Gervasi, B. Murgante, S. Misra, C. Garau, I. Blecic, D. Taniar, B.O. Apduhan, A. Rocha, E. Tarantino, C. M. Torre (Eds.), COMPUTATIONAL SCIENCE AND ITS APPLICATIONS, ICCSA 2021, PT X, vol. 12958, Springer International Publishing AG, Switzerland, 2021, pp. 19–32.
[64] U.K. Priya, R. Senthil, A review of the impact of the green landscape interventions on the urban microclimate of tropical areas, Build. Environ. 205 (2021) 108190, https://doi.org/10.1016/j.buildenv.2021.108190.
[65] S. Sen, J. Roesler, B. Ruddell, A. Middel, Cool pavement strategies for urban heat island mitigation in suburban Phoenix, Arizona, Sustainability 11 (2019) 4452, https://doi.org/10.3390/su11164452.
[66] Y. Li, S. Schubert, J.P. Kropp, D. Rybski, On the influence of density and morphology on the Urban Heat Island intensity, Nat. Commun. 11 (2020), https://doi.org/10.1038/s41467-020-16461-9.
[67] G. Guo, X. Zhou, Z. Wu, R. Xiao, Y. Chen, Characterizing the impact of urban morphology heterogeneity on land surface temperature in Guangzhou, China, Environ. Modell. Softw. 84 (2016) 427–439, https://doi.org/10.1016/j.envsoft.2016.06.021.
[68] Y. Wu, Y.J. Deng, Y.E. Gao, Z.L. Liang, Research on matching ability between trunk road network structure and urban spatial layout, Appl. Mech. Mater. 178–181 (2012) 1264–1278, https://doi.org/10.4028/www.scientific.net/AMM.178-181.1264.
[69] G. Del Serrone, P. Peluso, L. Moretti, Evaluation of microclimate benefits due to cool pavements and green infrastructures on urban heat islands, Atmosphere 13 (2022) 1586, https://doi.org/10.3390/atmos13101586.
[70] V.R.S. Cheela, M. John, W. Biswas, P. Sarker, Combating urban heat island effect—a review of reflective pavements and tree shading strategies, BUILDINGS-BASEL 11 (2021) 93, https://doi.org/10.3390/buildings11030093.
[71] Z. Shi, X. Zheng, Y. Chen, L. Liu, Implementation of “narrow road, dense network” plan in central area of jiangbei new district, nanjing, Planners 34 (2018) 129–134.
[72] F. Jiang, L. Ma, T. Broyd, K. Chen, H.B. Luo, Y. Pei, Sustainable road alignment planning in the built environment based on the MCDM-GIS method, Sust. Cities Soc. 87 (2022), https://doi.org/10.1016/j.scs.2022.104246.
[73] L. Tang, Q. Zhan, Y. Fan, H. Liu, Z. Fan, Exploring the impacts of greenspace spatial patterns on land surface temperature across different urban functional zones: a case study in Wuhan metropolitan area, China, Ecol. Indic. 146 (2023) 109787, https://doi.org/10.1016/j.ecolind.2022.109787.